

The crystal structure of braunite II and its relation to bixbyite and braunite

JOHAN P. R. DE VILLIERS

National Institute for Metallurgy
Applied Mineralogy Research Group
Department of Geology, Rand Afrikaans University
PO Box 524, Johannesburg, 2000, South Africa

Abstract

The crystal structure of braunite II, $\text{Ca}(\text{Mn,Fe})_{14}^{3+}\text{SiO}_{24}$, has been determined on a crystal from the Wessels Mine, near Hotazel, South Africa. It is tetragonal, space group $I4_1/acd$, with cell dimensions $a = 9.431(2)$, $c = 37.774(4)\text{\AA}$. The structure was refined by use of anisotropic thermal parameters and an extinction correction to a conventional $R = 0.058$. The structure consists of an $(A'ABA)_4$ stacking sequence of three non-equivalent edge- and corner-linked polyhedral sheets. The A- and A'-sheets consist of edge- and corner-linked (Mn,Fe) octahedra, whereas the B-sheets consist of Ca in cubic coordination, Si in tetrahedral coordination, and (Mn,Fe) in octahedral coordination. The A- and A'-sheets are present in bixbyite with stacking sequence $(A A')_2$, whereas the stacking sequence of braunite is $(AB)_4$. The A-, A', and B-sheets are virtually identical in the three structures. The structure determination confirms the validity of the braunite II structure as proposed previously. Comparative calculated X-ray diffraction data are presented so that distinctions can be made among these three minerals.

Introduction

The crystal structure of bixbyite has been the subject of recent investigations by Norrestam (1967) and Geller (1971). De Villiers (1975) and Moore and Araki (1976) examined the braunite structure and independently pointed out the very close relation between these two structures. Moore and Araki (1976) derive a theory that not only describes the braunite-bixbyite relation but also classifies all fluorite-structure derivatives. They also propose a structure for the compound first described by De Villiers (1946) as ferrian braunite and later designated as braunite II by De Villiers and Herbststein (1967).

This investigation is the continuation of a study of the crystal chemistry of economically important minerals from the Kalahari manganese field, Cape Province, South Africa. It also presents an opportunity to test the validity of the structure of braunite II as proposed by Moore and Araki (1976).

Experimental

A single crystal of braunite II was selected from specimens collected at the Wessels Manganese Mine, near Hotazel, Cape Province, South Africa. A part of

the type material has been deposited at the Royal Ontario Museum, Toronto, Canada, and is registered as M33733 and M34659. Braunite II occurs together with braunite and hausmannite as one of the predominant minerals in iron-rich portions of the mine. The composition given in Table 1 was determined by electron microprobe analysis using the Bence-Albee correction procedure, and was calculated on the basis of 24 oxygen atoms. Weight percentages of the constituent elements are 52.49 Mn, 10.63 Fe, 2.55 Si, and 3.03 Ca. Synthetic Mn_3O_4 (Mn), magnetite (Fe), and wollastonite (Ca,Si) were used as standards.

X-ray measurements with graphite-monochromated $\text{MoK}\alpha$ -radiation were completed on a roughly spherical crystal (see Table 1 for dimensions) that had been ground and mounted on a Philips PW1100 computer-controlled four-circle diffractometer. The cell dimensions were obtained from least-squares analysis of angular measurements of 44 reflections collected with a Stoe precision Weissenberg camera, and refined by use of a program by Burnham (1962).

The cell data are given in Table 1. The intensities of a unique set of reflections up to $\sin \theta/\lambda = 0.8$ were collected with the $\omega/2\theta$ scan technique, and the back-

Table 1. Crystal data for braunite II, composition $\text{Ca}_{0.92}(\text{Mn}_{11.72}\text{Fe}_{2.34})\text{Si}_{1.12}\text{O}_{24}$

a (Å)	9.431 (2)*
c (Å)	37.774 (4)
Space group	$I 4_1/acd$
Z	8
ρ calc (g. cm^{-3})	4.85
ρ obs	4.75
μ (cm^{-1})	111.34
Crystal diameter (cm)	0.018 ± 0.003
Number of reflections	
Observed	1300
Unobserved	889

Parenthesized figures represent the estimated standard deviated esd in terms of least units cited for the value to their immediate left, thus 9.431(2) indicates an esd of 0.002.

grounds were measured at the ends of each scan range. The systematically absent reflections uniquely defined space group $I4_1/acd$. Lorentz-polarization and spherical-absorption corrections were applied.

Table 2. Positional coordinates of the atoms in braunite II

Atom + Site symmetry	x	y	z
Ca 222 Ca	0	$\frac{1}{2}$	$\frac{1}{2}$
M(1) 2 $\text{Mn}_{0.83}\text{Fe}_{0.17}$	0	$\frac{1}{2}$	$-0.00918(3)^{++}$
M(2) 2 $\text{Mn}_{0.83}\text{Fe}_{0.17}$	0.2097(1)	0	$\frac{1}{2}$
M(3) 2 $\text{Mn}_{0.83}\text{Fe}_{0.17}$	0.2408(1)	$\frac{1}{4}+x$	$\frac{1}{2}$
M(4) 1 $\text{Mn}_{0.83}\text{Fe}_{0.17}$	0.0312(1)	0.0006(1)	0.06290(2)
M(5) 1 $\text{Mn}_{0.83}\text{Fe}_{0.17}$	-0.0096(1)	0.0044(1)	0.18772(2)
Si 4 Si	0	$\frac{1}{2}$	$\frac{3}{8}$
O(1) 1	0.1197(4)	0.1715(5)	0.0256(1)
O(2) 1	0.3314(5)	0.4010(5)	0.0311(1)
O(3) 1	0.3982(4)	0.1227(5)	0.0412(1)
O(4) 1	0.1178(4)	0.4071(4)	0.0879(1)
O(5) 1	0.1701(5)	0.1121(5)	0.0909(1)
O(6) 1	0.3874(5)	0.3361(5)	0.1004(1)

Extinction parameter $g = 1.62(8) \times 10^{-3}$

* Origin based on centre of symmetry

++ Estimated standard errors in parentheses refer to the last digit.

Table 3. Thermal parameters in Å^2 ($\times 10^4$) for the atoms in braunite II

Atom	$U^*_{(11)}$	$U_{(22)}$	$U_{(33)}$	$U_{(12)}$	$U_{(13)}$	$U_{(23)}$
Ca	44(5)	$U_{(11)}$	55(7)	-3(8)	0	0
M(1)	74(5)	103(6)	63(3)	29(5)	0	0
M(2)	63(5)	94(5)	74(4)	0	0	25(4)
M(3)	73(3)	$U_{(11)}$	63(3)	1(4)	-5(3)	$-U_{(13)}$
M(4)	57(3)	69(3)	77(3)	7(3)	5(2)	-17(3)
M(5)	46(3)	60(3)	62(3)	-6(3)	-2(3)	-2(3)
Si	49(7)	$U_{(11)}$	57(10)	0	0	0
O(1)	108(18)	106(18)	67(15)	30(15)	-11(14)	8(14)
O(2)	71(18)	76(17)	66(15)	-7(14)	12(14)	13(14)
O(3)	37(16)	97(19)	112(16)	-7(14)	19(14)	44(14)
O(4)	57(17)	57(16)	61(15)	-13(13)	-22(13)	28(13)
O(5)	67(17)	83(18)	52(15)	6(14)	-12(14)	21(14)
O(6)	77(18)	95(18)	64(15)	1(15)	-3(14)	-3(14)

* The form of the anisotropic temperature factor is

$$T = \exp -2\pi^2 (a^{*2}h^2U_{11} + b^{*2}k^2U_{22} + c^{*2}l^2U_{33} + 2\alpha^*b^*hkU_{12} + 2\alpha^*c^*hlU_{13} + 2b^*c^*klU_{23}).$$

The significance level of 5 percent was the criterion for the determination of unobserved reflections ($I \leq 1.65\sigma I$), where I is the observed intensity. The X-ray system of programs was used for all crystallographic calculations (Stewart *et al.*, 1972).

From a three-dimensional Patterson map, a unique solution for the cation positions was obtained. When these cations were used as the input to a Fourier program, the oxygen positions could not be determined because of severe pseudosymmetry in the Fourier map. The correct atomic positions for cations and oxygen were obtained by direct methods using tangent iteration. The reflections 6, 2, 8; 8, 4, 16; 4, 4, 16; and 8, 5, 19 were used as starting phases. The reason for the severe pseudosymmetry on the Fourier map is that the correct positions of cations M1, M2, M3, M4, and M5 are slightly offset from their highly symmetric positions at $0, \frac{1}{4}, 0; \frac{1}{4}, 0, \frac{1}{4}; \frac{1}{4}, \frac{1}{2}, \frac{1}{8}; 0, 0, \frac{1}{16}$; and $0, 0, \frac{3}{16}$, respectively, as determined from the Patterson peaks. These shifts are in different directions, depending on the origin specified. As a result, correct Fourier phasing cannot take place since the symmetric starting positions are the mean of all possible shifts that depend on the different choices of origin.

Refinement of the structure with starting atomic positions obtained from tangent iteration proceeded normally. The quantity minimized is $R(F) = \Sigma W(|F_o| - |F_c|)^2$. Scattering factors of neutral atoms were obtained from *International Tables*, Vol. III. The final four cycles included an anomalous dispersion

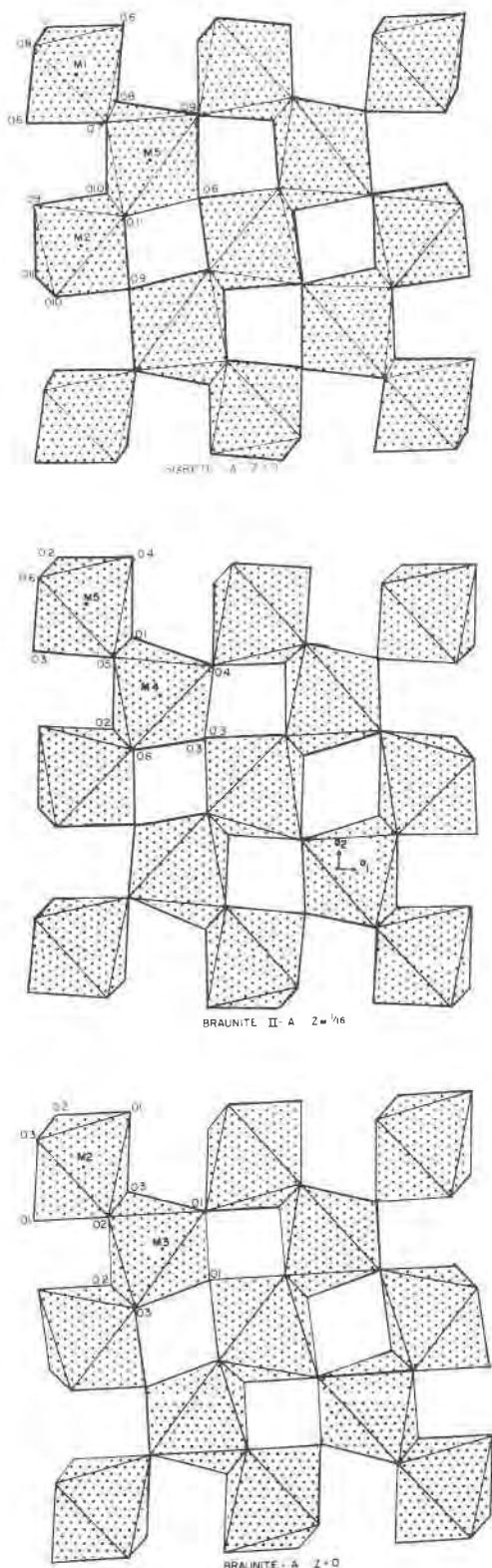


Fig. 1. The A-sheets of octahedra in α - Mn_2O_3 , braunite II, and braunite. The axes of braunite II are shown for comparison. Unique atoms are labelled.

correction, one scale factor, one secondary extinction parameter (Larson, 1967), together with positional and anisotropic thermal parameters for all atoms. At convergence, $R = 0.058$ and $R_w = 0.053$ for 1300 observed reflections. Final positional parameters and the secondary extinction parameter with their standard deviations are given in Table 2. The anisotropic thermal parameters are given in Table 3, the interatomic distances and angles in Table 4, and observed and calculated structure factors are compared in Table 6.¹

Relation between bixbyite and braunite

In their comparison of bixbyite and braunite, Moore and Araki (1976) identified three different types of polyhedral sheets, designated the A-, A'-, and B-sheets. The A- and A'-sheets consist of edge- and corner-linked octahedra. In cubic bixbyite these sheets are equivalent, but in orthorhombic α - Mn_2O_3 they are not. The B-sheets in braunite consist of Mn^{2+} in distorted cubic coordination, Mn^{3+} in octahedral coordination, and Si^{4+} in tetrahedral coordination.

The braunite II structure contains all three types of sheets, *i.e.* A, A', and B, in a regular stacking arrangement.

In Figure 1, comparison of the A-sheets of α - Mn_2O_3 , braunite II, and braunite shows that the sheets are isomorphic in all respects except for minor dimensional differences in the polyhedra. The unique atoms are labelled in each of the three sheets. The labelling of the atoms corresponds to that of Geller (1971) in the $Pbca$ orientation for α - Mn_2O_3 , that of De Villiers (1975) for braunite, and that of braunite II in the present study.

In Figure 2, the A'-sheets of α - Mn_2O_3 and braunite II are shown. In order that the braunite II structure can be compared directly with Mn_2O_3 and braunite, the braunite II sheets with z-coordinates indicated are rotated by 90 degrees and the origin is shifted to $1/4, 1/4, 0$. This gives direct correspondence of the sheets indicated in Figures 1, 2 and 3. The a_1 and a_2 axes are shown on the sheets of braunite II.

In Figure 3, the B-sheets of braunite II and braunite are shown for purposes of comparison, and it can be seen that the (CaO_8) cube in braunite II is less distorted than the $[M(1)O_8]$ cube in braunite.

¹ To receive a copy of this material, order Document AM-80-126 from the Business Office, Mineralogical Society of America, 2000 Florida Avenue, N.W., Washington, D.C. 20009. Please remit \$1.00 in advance for the microfiche.

The stacking sequences of these structures are diagrammatically illustrated in Figure 4. From this figure, the stacking sequences derived and postulated by Moore and Araki (1976) can be easily deduced: bixbyite with $(A A')_2$, braunite with $(AB)_4$, and braunite II with $(A' ABA)_4$.

Coordination polyhedra

Figures 1, 2, and 3 show that the Ca atom is in distorted cubic coordination, Si is in tetrahedral coordination, and the 5 M atoms, (Mn,Fe) are in octahedral coordination with varying degrees of distortion.

As can be seen from Table 4, the Ca atom is coordinated *via* four long and four short Ca–O bonds giving an average of 2.378 Å. This deviates markedly from the value of 2.50 Å derived from the ionic radii for Ca^{VIII} and O^{IV} atoms given by Shannon and Prewitt (1969). However, these authors indicated that in the fluorite structure, of which braunite II is a derivative, the Ca^{2+} ionic radius is probably too large by 0.06 Å. If the ionic radius of Ca^{2+} in braunite II is assumed to be 1.06 Å, a bond length of 2.44 Å is obtained, which is in closer agreement with the observed average. There is still a discrepancy of 0.06 Å, possibly due to a more efficient packing of O-atoms in a twisted cubic coordination. However, it seems that the CaO_8 cube, in which all edges are shared, has an effective radius differing from that of Ca in other 8-coordinated environments.

The O–Ca–O angles vary from 65° to 75.7° as compared to the value of 70.5° in a regular cube. The O–M(1)–O angles in braunite vary from 62° to 77.5°.

The cube in braunite II is therefore more regular than that in braunite.

The average octahedral bond lengths of M(1)–O, 2.043 Å; M(2)–O, 2.049 Å; M(3)–O, 2.038 Å; M(4)–O, 2.053 Å; and M(5)–O, 2.021 Å compare well with the value of Mn^{3+} –O = 2.05 derived from Shannon and Prewitt (1969).

With the exception of M(5), all the octahedra show marked elongation that could be attributed to Jahn–Teller distortion, although the magnitude of this distortion is not predicted by this theorem. If it is assumed that the elongation is due to Jahn–Teller distortion around Mn^{3+} , the reason for the more equidistant bonds round M(5) could be the occupancy of most of the Fe^{3+} at this site. Approximately half of the site will be occupied by Fe^{3+} . The relatively short average bond length of 2.021 Å is explained by the theorem of Brown (1978), which states that any deviation of bond lengths from their average value will increase the average bond length. The more regular M(5) octahedron must therefore have a shorter average bond length.

A measure of the distortion of the octahedra is given by the apical O–M–O angles, which deviate from 180 degrees when distortion occurs. As in braunite (Moore and Araki, 1976), two types of octahedra are also present in braunite II, and are shown schematically in Figure 5. Octahedra M(1), M(2), and M(4) belong to the distorted type with apical angles of 138°, 139°, and 139° respectively, as the maximum deviation from regularity. The M(3) and M(5) octahedra show angles of 177° and 172° respectively.

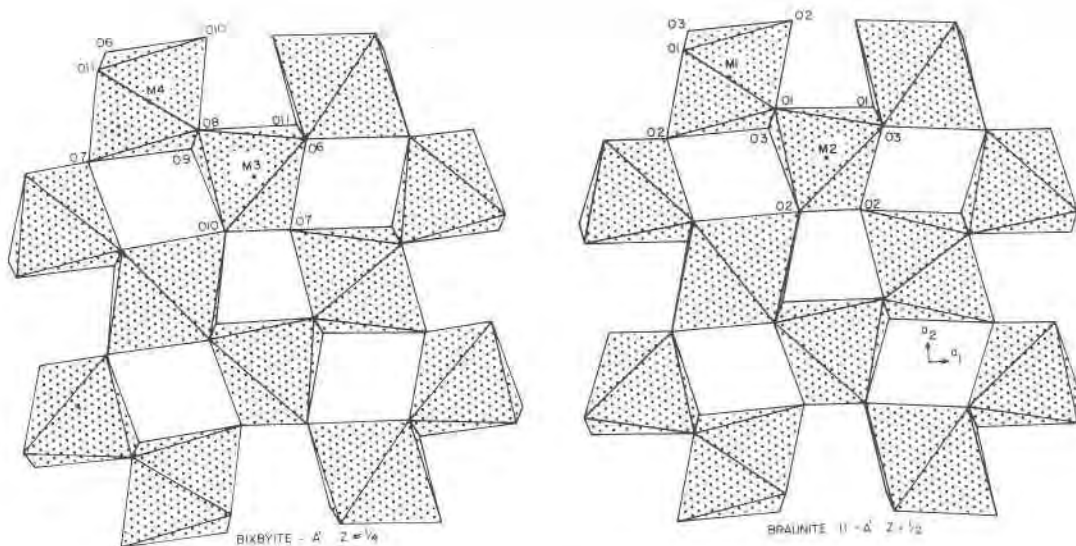


Fig. 2. The A'-sheets of octahedra of $\alpha\text{-Mn}_2\text{O}_3$ and braunite II. Unique atoms are labelled.

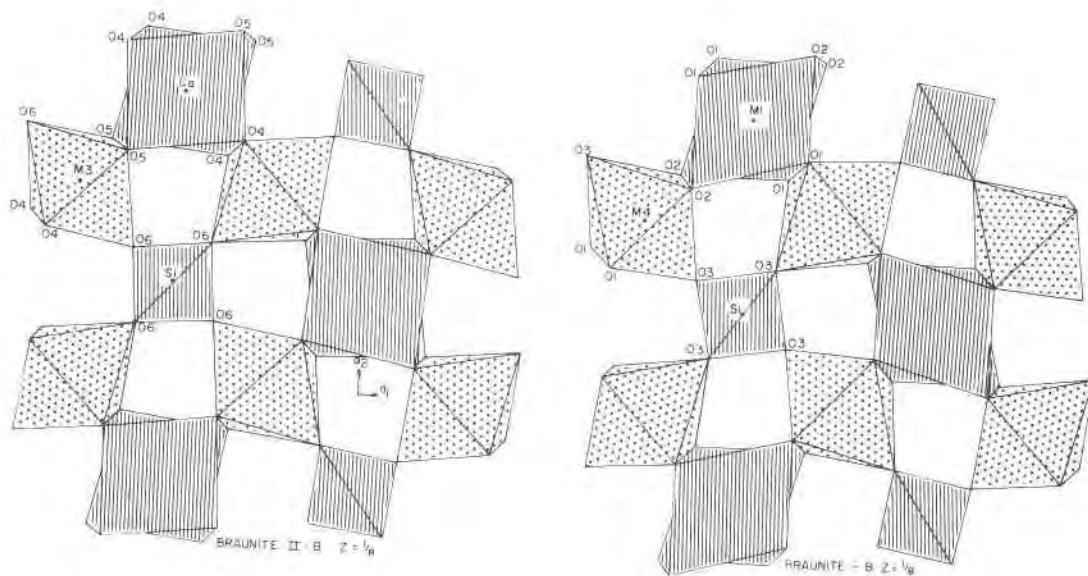


Fig. 3. The B-polyhedral sheets of braunite II and braunite. The twisted cubic Ca-polyhedra as well as the Si-tetrahedra are shown with M-octahedra.

Bixbyite c = 9.403	Braunite II c = 37.774	Braunite c = 18.703
	*** 0 A'	
xxxxx 0 A	xxxxx ¹ / ₁₆ A	xxxxx 0 A
*** ¹ / ₄ A'	+++ ¹ / ₈ B	+++ ¹ / ₈ B
xxxxx ¹ / ₂ A	xxxxx ³ / ₁₆ A	xxxxx ¹ / ₄ A
*** ³ / ₈ A'	*** ¹ / ₄ A'	+++ ⁵ / ₈ B
xxxxx 0 A	xxxxx ⁵ / ₁₆ A	xxxxx ¹ / ₂ A
	+++ ⁵ / ₈ B	+++ ⁵ / ₈ B
	xxxxx ⁷ / ₁₆ A	xxxxx ³ / ₄ A
	*** ¹ / ₂ A'	+++ ⁷ / ₈ B
	xxxxx ⁹ / ₁₆ A	xxxxx 0 A
	+++ ⁵ / ₈ B	
	xxxxx ¹¹ / ₁₆ A	
	*** ³ / ₄ A'	
	xxxxx ¹³ / ₁₆ A	
	+++ ⁷ / ₈ B	
	xxxxx ¹⁵ / ₁₆ A	
	*** 0 A'	

† xxx denotes the A layer (Figure 1)
 *** denotes the A' layer (Figure 2)
 +++ denotes the B layer (Figure 3)

Fig. 4. Stacking sequences† in bixbyite, braunite II, and braunite.

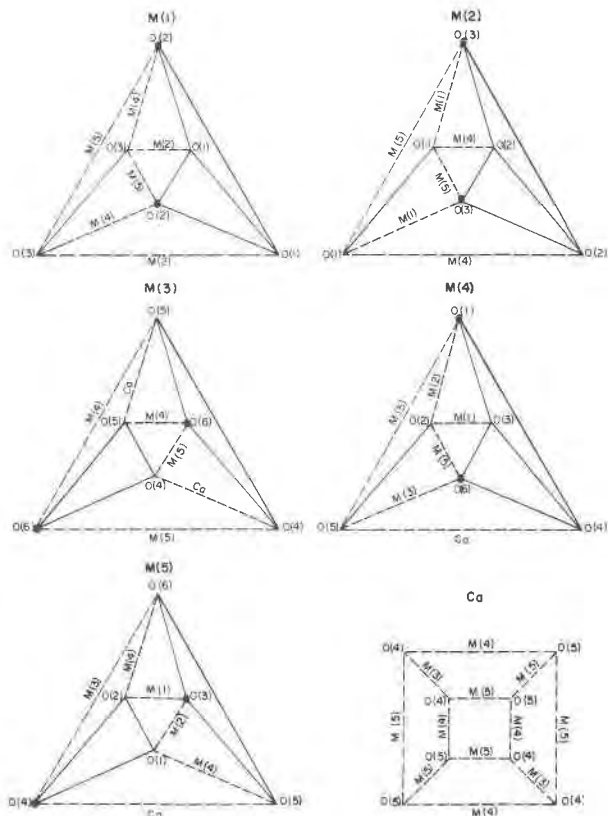


Fig. 5. Polyhedral diagrams showing the distribution of shared edges of polyhedra. The cation polyhedron, with which an edge is shared, is also listed. Shared edges are delineated by dashes, and elongated apical bonds by enlarged dots.

Table 5. Calculated atomic valences for atoms in braunite and braunite II

Braunite		Braunite II		
Atom	Valence	Atom	Valence (*)	(**)
M(1)	2.02	Ca	2.47	2.03
M(2)	3.05	M(1)	3.05	3.05
M(3)	2.88	M(2)	2.86	2.86
M(4)	2.97	M(3)	2.93	2.93
Si	4.02	M(4)	2.90	2.90
O(1)	1.89	M(5)	2.96	2.96
O(2)	2.07	Si	3.93	3.93
O(3)	2.00	O(1)	1.97	1.97
		O(2)	1.96	1.96
		O(3)	1.94	1.94
		O(4)	1.96	1.91
		O(5)	2.12	2.06
		O(6)	1.95	1.95

* Bond valences according to formula (1)

** Bond valences of Ca-O according to formula (2)

As Moore and Araki (1976) have pointed out, the distribution of shared polyhedral edges along one side of the polyhedra of the first kind causes cation-to-cation repulsion, whereas $2/m$ pseudosymmetry in the second kind of octahedra results in a less distorted environment. The distortions in the so-called meridional bonds will be discussed below. The SiO_4 tetrahedron is nearly regular, with angles of 109.0° and 110.3° , which are close to the theoretical 109.3° .

Bond-valence calculations

In an attempt to explain the variations of bond lengths, the method of Brown and Wu (1976) was employed for calculation of cationic and anionic va-

lence sums for all atoms in braunite and braunite II. With this method the valence of each cation-to-oxygen bond can be calculated. These valences are summed for all bonds around each of the atoms, yielding an experimental valence for each atom. The formula used was

$$s = (R/R_1)^{-N} \quad (1)$$

where s is the bond valence, R the experimentally determined bond distance, and R_1 and N are constants given by Brown and Wu (1976). The anomalous Ca-O distances gave a very poor valence sum for Ca, since the values for R_1 and N in this method are based on Ca-O distances larger than those in braunite II. The alternative formula in the same publication was therefore used, namely,

$$s = \bar{s}(\bar{R}/R)^{-(0.6r+2.2)} \quad (2)$$

where \bar{s} and \bar{R} are the average bond valence and bond lengths respectively, and ν is the coordination number for the cation. This formula was used only in the case of the Ca atom. The results are given in Table 5.

Moore and Araki (1976) postulated that the splitting of meridional bonds of M(2) in braunite is due to undersaturation of 0.25 valence units for O(1), and oversaturation of 0.25 valence units for O(3). From the values given in Table 5, the slight undersaturation of 0.11 v.u. for O(1) could account for the short M(2)-O(1) bonds.

With regard to braunite II, the splitting in meridional bonds are M(1), 0.073 Å; M(2), 0.070 Å; M(3), 0.064 Å; M(4), 0.013 Å; and M(5), 0.123 Å. The split-

Table 7. Cell parameters of bixbyite, braunite, and braunite II

	Bixbyite		Braunite		Braunite II
	(a)	(b)	(a)	(b)	
\underline{a} (Å) :	9.4157(3)*	9.4146(1)	9.4248(2)	9.425(1)	9.431(2)
\underline{b} (Å) :	9.4233(3)	-	-	-	-
\underline{c} (Å) :	9.4047(3)	-	18.6989(9)	18.700(3)	37.774(4)
Space group:	$Fo\bar{a}b$	$Ia\bar{3}$	$I4_1/acd$	$I4_1/acd$	$I4_1/acd$
Z :	16		8		8
Composition:	(a) Mn_2O_3		(a) $(\text{CaMgMn})^{2+}(\text{Mn,Fe})_6^{3+}\text{SiO}_{12}$	$\text{Ca}(\text{Mn,Fe})_{14}^{3+}\text{SiO}_{24}$	
	(b) $(\text{Mn}_{0.98}\text{Fe}_{0.02})_2\text{O}_3$		(b) $\text{Mn}^{2+}\text{Mn}_6^{3+}\text{SiO}_{12}$		
References :	Geller (1971)		(a) This study	This study	
			(b) Abs-Wurbach and Langer (1975)		

* Parenthesized figures represent the estimated standard errors in terms of least units cited for the value to their immediate left, thus 9.4157(3) indicates an estimated standard error of 0.0003.

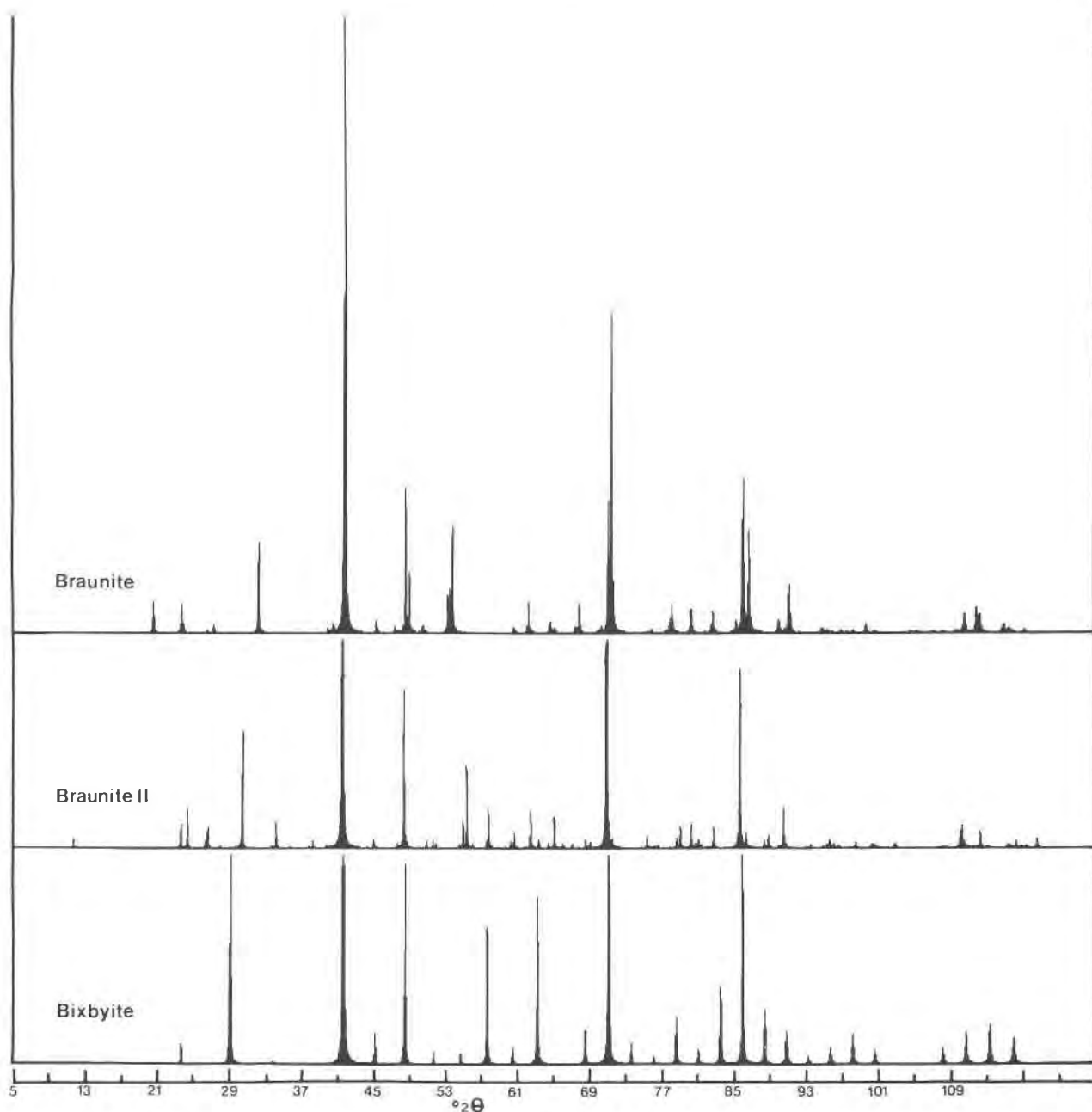


Fig. 6. Comparison of calculated X-ray diffraction data of bixbyite, braunite II, and braunite ($\text{FeK}\alpha$).

ting of 0.123\AA in M(5) cannot be explained on the basis of valence sums of oxygen atoms. However, the octahedron is not elongated in the same sense as the others, so that it is difficult to decide the nature of the meridional bonds. Alternatively, the octahedron could be described as a compressed octahedron due to Jahn–Teller distortion. The splitting of meridional bonds is then only 0.036\AA .

Appendix

Calculated X-ray powder patterns of bixbyite, braunite and braunite II

Introduction

The identification of bixbyite, braunite, and braunite II has presented problems for some time.

Table 8. X-ray diffraction data for bixbyite, braunite, and braunite II

Bixbyite	Braunite	Braunite II	Bixbyite	Braunite	Braunite II	
2 0 0	4.707(2)	1 1 2 5.427(2)	0 0 8 4.722(1)	0 2 6 } 6 2 0 }	1.4886(2)	4 1 19 1.5005(3)
2 1 1	3.843(18)	2 0 0 4.712(2)	2 0 0 4.716(1)	1 4 5 } 5 4 1 }	1.4527(7)	5 4 3 1.4629(2)
2 2 2	2.718(100)	2 1 3 3.492(7)	2 0 4 4.219(1)	6 2 2	1.4193(21)	2 2 24 1.4233(9)
3 2 1 } 1 2 3 }	2.516(2)	2 2 4 2.713(100)	2 1 1 4.192(1)	6 3 1 } 1 3 6 }	1.4115(11)	6 2 8 1.4219(16)
4 0 0	2.354(15)	3 1 4 2.513(1)	2 1 5 3.683(8)	4 4 4	1.3881(6)	6 1 11 1.4131(2)
4 1 1	2.219(1)	4 0 0 2.356(11)	1 1 10 3.287(2)	6 3 3 1.3706(2)	6 3 5 1.3822(2)	
4 2 0 } 0 2 4 }	2.105(1)	0 0 8 2.337(5)	2 2 8 2.724(100)	4 4 8 1.3567(5)	4 4 16 1.3618(5)	
3 3 2	2.007(11)	3 3 2 2.161(3)	0 0 16 2.361(5)	3 3 3 1.3056(2)	7 2 3 1.2675(1)	
4 2 2	1.9217(2)	3 1 6 2.154(4)	4 0 0 2.358(11)	1 2 7 }	1.2812(3)	
4 3 1 } 1 3 4 }	1.8464(14)	3 2 5 2.142(8)	3 3 6 2.096(2)	2 4 6	1.2581(2)	
5 2 1 } 1 2 5 }	1.7189(3)	0 0 2 2.081(7)	3 2 11 2.001(3)	6 5 1 } 7 3 2 }	1.1957(2)	
4 4 0	1.6643(37)	3 3 10 1.9158(2)	4 3 3 1.8654(3)	8 0 0	1.1768(4)	0 0 32 1.1804(2)
4 3 3	1.6146(2)	4 3 1 1.8755(3)	4 1 13 1.7973(3)	8 0 0 1.1687(3)	8 1 1 1.1667(2)	8 1 3 1.1648(2)
5 3 2 } 6 1 1 } 2 3 5 }	1.5272(5)	5 1 2 1.8133(1)	4 0 16 1.6683(28)	7 4 1 } 1 4 7 }	1.1589(6)	
		4 1 7 1.7368(3)	4 4 0 1.6672(13)	8 1 1 }	1.1417(4)	6 5 5 1.1484(1)
		4 4 0 1.6661(12)	4 3 13 1.5821(1)	8 2 0 } 0 2 8 }	1.1253(5)	6 5 11 1.1391(1)
		4 0 8 1.6594(30)	5 1 14 1.5255(1)	6 5 3 } 3 5 6 }		
		4 3 7 1.5401(1)	6 1 5 1.5188(2)			
		4 1 9 1.5375(3)				
		6 1 3 1.5037(3)				

The publication of De Villiers and Herbstein (1967) clarified the position regarding the identification of these minerals and supplied some diffraction data. However, the X-ray diffraction patterns published in the JCPDS powder-diffraction file still contain misleading information; for example, the pattern for braunite is a composite of data from several investigators, and is labelled as *disordered braunite*, which it obviously is not. The pattern for braunite II is only partially indexed.

After the braunite and braunite II crystal structures were solved, it was decided that their X-ray diffraction data should be compared with those of bixbyite as an aid to the identification of these very similar minerals.

Unit-cell data

The unit-cell data for bixbyite are taken from Geller (1971). Because of the discrepancies in the cell data for braunite of De Villiers (1975), Abs-Wurmbach and Langer (1975), and Moore and Araki (1976), the cell parameters in this study were refined on material from Långban, Sweden. De Villiers (1975) gives its composition. The 53 angular values obtained by powder diffractometry, and corrected by use of a silicon internal standard, were used in the least-squares program by Appleman and Evans (1973). Cell parameters for all three minerals are given in Table 7.

X-ray diffraction data

For precise indexing, the diffraction patterns, especially of braunite II, were calculated with the aid of the program POWD7 (Smith and Holomany, 1978). Cell data, atomic parameters, and compositions of Geller (1971), De Villiers (1975), and this study were used for bixbyite, braunite, and braunite II respectively. Comparison of the calculated and observed patterns showed that they are virtually indistinguishable in all cases. This illustrates the ability of the program to render unequivocal characterization of complex X-ray powder-diffraction patterns.

The calculated patterns for the three minerals are shown in Figure 6 and the indexed major calculated reflections in Table 8. The wavelength used in all calculations is $\text{FeK}\alpha$. The major peaks in the three patterns have been truncated in Figure 6 so that the minor peaks can be seen more distinctly. For the intensity values of the peaks shown in Figure 6, refer

to Table 8. The similarity in the patterns is immediately evident in Figure 6, which also shows the diagnostic reflections quite clearly.

Acknowledgments

This paper is published by permission of the President of the National Institute for Metallurgy. I thank Dr. G. Gafner, Dr. G. J. Kruger, Dr. J. Coetzer, and Dr. J. C. A. Boeyens of the South African Council for Scientific and Industrial Research for data collected and valuable discussions; Mr. E. A. Viljoen of the National Institute for Metallurgy for microprobe analysis; and Mr. J. J. Taljaardt of S. A. Manganese Amcor Ltd. for providing samples.

References

- Abs-Wurmbach, I. and K. Langer (1975) Synthetic Mn^{3+} -kyanite and viridine, $(\text{Al}_{2-x}\text{Mn}_x^{3+})\text{SiO}_3$, in the system Al_2O_3 - MnO - MnO_2 - SiO_2 . *Contrib. Mineral. Petrol.*, 49, 21-38.
- Appleman, D.E. and H. T. Evans Jr. (1973) Job 9214: Indexing and least squares refinement of powder diffraction data. *Natl. Tech. Inf. Serv., U.S. Dep. Commerce, Springfield, Virginia, Document PB-216188*.
- Brown, I.D. (1978) Bond valences—a simple structural model for inorganic chemistry. *Chem. Soc. Rev.*, 7, 3, 359-376.
- and K.K. Wu (1976) Empirical parameters for calculating cation-oxygen bond valences. *Acta Crystallogr.*, B32, 1957-1959.
- Burnham, C.W. (1962) Lattice constant refinement. *Carnegie Inst. Wash. Year Book*, 61, 132-135.
- De Villiers, J.E. (1946) Some minerals occurring in South African manganese deposits. *Geol. Soc. S. Afr. Trans.*, 48, 17-25.
- De Villiers, J.P.R. (1975) The crystal structure of braunite with reference to its solid solution behaviour. *Am. Mineral.*, 60, 1098-1104.
- De Villiers, P.R. and F.H. Herbstein (1967) Distinction between two members of the braunite group. *Am. Mineral.*, 52, 20-30.
- Geller, S. (1971) Structures of α - Mn_2O_3 , $(\text{Mn}_{0.983}\text{Fe}_{0.017})_2\text{O}_3$ and $(\text{Mn}_{0.37}\text{Fe}_{0.63})_2\text{O}_3$ and relation to magnetic ordering. *Acta Crystallogr.*, 27, 821-828.
- Larson, A.C. (1967) Inclusion of secondary extinction in least-squares calculations. *Acta Crystallogr.*, 23, 664-665.
- Moore, P.B. and T. Araki (1976) Braunite: its structure and relationship to bixbyite, and some insights on the genealogy of fluorite derivative structures. *Am. Mineral.*, 61, 1226-1240.
- Norrestam, R. (1967) α -Manganese (III) oxide—a C-type sesquioxide with orthorhombic symmetry. *Acta Chem. Scandinavica*, 21, 2871-2884.
- Shannon, R.D. and C.T. Prewitt (1979) Effective ionic radii in oxides and fluorides. *Acta Crystallogr.*, 25, 925-946.
- Smith, D.K. and M. Holomany (1978) A FORTRAN IV program for calculating X-ray powder diffraction patterns—Version 7. *Pennsylvania State University, Department of Geosciences*.
- Stewart, J.M., G.J. Kruger, H.L. Ammon, C. Dickinson and S.R. Hall (Eds.) (1972) The X-ray system of crystallographic programs. *Tech. Rep. 192, Computer Science Center, University of Maryland*.

Manuscript received, July 12, 1979;
accepted for publication, November 24, 1979.